Image Denoising Using Adaptive Thresholding in Wavelet Domain

Yogendra Singh, Mr. Avinash Rai
Department of Electronics and Communication Engineering,
University Institute of Technology, Rajiv Gandhi Proudyogiki Vishwavidyalaya

Abstract -Visual information transmitted in the form of digital images is becoming a major method of communication in the modern age, but the image obtained after transmission is often corrupted with noise. Noise is unwanted signal that interferes with the original signal and degrades its visual quality. The received image needs processing before it can be used in applications. Image denoising involves the manipulation of the image data to produce a visually high quality image. Denoising method tends to be problem specific and depends upon the type of image and noise model. Wavelet transforms have been widely used for image denoising since they provide a suitable basis for separating noisy signal from the image signal. A novel image denoising method based on wavelet transforms to preserve edges is described in this paper. The decomposition is performed by dividing the image into a set of blocks and transforming the data into the wavelet domain. An adaptive thresholding scheme based on edge strength is used to effectively reduce noise while preserving important features of the original image. Experimental results, compared to other approaches, demonstrate that the proposed method suitable for different classes of images contaminated by Gaussian noise.

Keywords- Digital images, Adaptive Thresholding & Wavelet Domain.

I. INTRODUCTION

Visual information transmitted in the form of digital images is becoming a major method of communication in the modern age, but the image obtained after transmission is often corrupted with noise. Noise is unwanted image that interferes with the original image and degrades its visual quality. The received image needs processing before it can be used in applications. Image denoising involves the manipulation of the image data to produce a visually high quality image. Denoising method tends to be problem specific and depends upon the type of image and noise model. Image denoising is an essential work in image processing, using of wavelets improves the quality of an image and reduces noise level [1]. Owing to denoising rapidly increasing popularity over last few decades, the wavelet transform has become quite a standard tool in numerous research and application domains. This paper is about wavelet domain image denoising. In general, image denoising imposes a accord between reduction of noise and preserving important image details [2]. The wavelet representation characteristically encourages the development of such spatially versatile calculations. It layers the fundamental data in a sign into moderately few, extensive coefficients, which speak to picture points of interest at diverse determination scales.

The central idea to wavelets is to analyze according to scale. Imagine a function that oscillates like a wave in a limited portion of time or space and vanishes outside of it. The wavelets are such functions: wave-like but localized. One chooses a particular wavelet, stretches it and shifts it, while looking into its correlations with the analyzed image. This analysis is similar to observing the displayed image from various distances. The image correlations with wavelets stretched to large scales reveal gross features, while at small scales fine image structures are discovered. It is therefore often said that the wavelet analysis is to see both the forest and the trees. The origins of the wavelet analysis can be traced to the 1909 Haar wavelet and various “atomic decompositions” in the history of mathematics. The current use of the name “wavelet “is due to Grosman's and Morlet's work on geophysical image processing, which led to the formalization of the continuous wavelet transform. In the development of wavelets, the ideas from many different fields have merged.[3]

Image processing

An image may be defined as a two-dimensional (2D) function, f(x, y), where x and y are *plane* co-ordinates, and the amplitude of f at any pair of coordinates (x, y) is called the *intensity* or *gray level* of the image at that point. When x, y, and the amplitude values of f are all finite, discrete quantities, we call the image a *digital image*. The field of *digital image processing* refers to processing digital images by means of a digital computer. Note that a digital image is composed of a finite number of elements, each of which has a particular location and value. These elements are referred to as *picture elements*, *image elements*, *pels*, and *pixels*. *Pixel* is the term most widely used to denote the elements of a digital image [2]. Vision is the most advanced of our senses, so it is not surprising that images play the single most important role in human perception. However, unlike humans, who are limited to the visual band of the electromagnetic (EM) spectrum, imaging machines cover almost the entire EM spectrum, ranging from gamma to radio waves. They can operate on images

generated by sources that humans are not accustomed to associating with images. These include ultrasound, electron microscopy, and computer-generated images. Thus, digital image processing encompasses a wide and varied field of applications.

Noise

Noise is undesired information that contaminates the image. In the image denoising process, information about the type of noise present in the original image plays a significant role.

Typical images are corrupted with noise modeled with either a Gaussian, uniform, or salt or pepper distribution. Another typical noise is a speckle noise, which is multiplicative in nature.[4]

Noise is present in an image either in an additive or multiplicative form

An additive noise follows the rule

$$w(x, y) = s(x, y) + n(x, y) \quad (1.1)$$

while the multiplicative noise satisfies

$$w(x, y) = s(x, y) \times n(x, y) \quad (1.2)$$

where $s(x,y)$ is the original image, $n(x,y)$ denotes the noise introduced into the image to produce the corrupted image $w(x,y)$, and (x,y) represents the pixel location. The above image algebra is done at pixel level. Image addition also finds applications in image morphing. By image multiplication, we mean the brightness of the image is varied.

The digital image acquisition process converts an optical image into a continuous electrical image that is, then, sampled . At every step in the process there are fluctuations caused by natural phenomena, adding a random value to the exact brightness value for a given pixel.

II. DISCRETE WAVELET TRANSFORM

Mathematically, either in time domain or in spatial domain, we can represent a wave in terms of a sinusoidal function. By applying Fourier analysis any random image can be expressed in the form of sinusoidal function of infinite harmonics. In comparison of sinusoidal function , wavelets can be treated as small waves that concentrates energy in time domain .[8] On wavelet, together we can apply frequency and time analysis, since it closely resembles the structure of a wave, and here mainly energy is contained in time domain.

Introduction to Wavelet Transforms

Wavelets are functions can be generated using basis function called mother wavelet by dilations (scaling) and translations (shifts) in frequency domain or time domain.[9]

Let the mother wavelet = $\Psi(t)$
We can represent other wavelet = $\Psi_{a,b}(t)$

$$\Psi_{a,b}(t) = \frac{1}{\sqrt{a}}\Psi\left(\frac{t-b}{a}\right) \quad (2.1)$$

Where
a and b = two random real numbers.
a = variable for dilation
b = variable for translation

From Eq. 2.1 we can express a mother wavelet as shown below

$$\Psi(t) = \Psi_{1,0}(t) \quad (2.2)$$

When

$a \neq 1$ & $b=0$,then

$$\Psi_{a,b}(t) = \frac{1}{\sqrt{a}}\Psi\left(\frac{t-b}{a}\right) \quad (2.3)$$

Eq. 2.3, indicates that $\Psi_{a,0}(t)$is scaling in time by an amount a and scaling in amplitude by an amount $\sqrt{a}$ version of the mother wavelet function in Eq. 2.2[10].

When

$a < 1$ = indicates shrink (contraction) in $\Psi(t)$

$a > 1$ = indicates expansion in $\Psi(t)$

$a < 0$ = it means time reversal with scaling in $\Psi(t)$

hence a is either known as dilation or scaling variables.

In eq. 2.3, when 't' is replaced by 't-b' then it shows $\Psi_{a,b}(t)$ the wavelet function gets translated or shifted in time axis as in eq. 2.1

When

$b>0$ = it indicates $\Psi_{a,0}(t)$ is a shift of $\Psi(t)$ towards right by an amount b along time axis

$b<0$ = it indicates $\Psi_{a,0}(t)$ is a shift of $\Psi(t)$ towards left by an amount b along time axis

hence variable b is popularly known as translation variable[11]

III. PROPOSED METHODOLOGY

In conventional thresholding schemes, a global (universal) threshold is commonly used to filter small wavelet coefficients. However, this procedure can also remove high frequency components, such as edges. To improve the wavelet denoising method, an adaptive threshold is calculated in a subband-dependent manner to characterizelocal features of the image. A new thresholding scheme is proposed to threshold the small wavelet coefficients considered to be noise while preserving edges. This sub and- dependent thresholding is obtained based on the calculation of noise level and edge strength. The main stages of the proposed wavelet denoising method are illustrated in Fig. 1.

Initially, the input image g, corrupted by Gaussian noise, is partitioned into m × m pixel blocks. Blocks are used in a manner such that the denoising algorithm can exploit local noise characteristics and adapt thresholding to produce better results. Nevertheless, as information is often lost due to the thresholding, blocking effects between boundaries of neighbor blocks often arise. A larger region Bn of size n × n pixels (n>m), encompassing an m × m block Bm, is used to avoid such undesirable effects. The discrete wavelet transform is then applied to each block Bn.[9]

An edge detection algorithm is used to identify edges in the image. A multiscale edge detection based on Haar wavelet transform modulus maxima is used for this purpose [12], being applied separately to each block. In order to have a precise edge localization and avoid noise, after applying the edge detection, each coefficient identified as edge information is compared to its neighbors. If there isno neighbor belonging to an edge, the coefficient is nolonger identified as edge information. The multiscale edgedetection produces an edge map for each subband, that is, abinary image where 1 represents an active edge elementand 0 represents a non-edge element.

The threshold on a given subband i is given by

$$\lambda_i = \frac{\hat{\sigma}^2_{noise}}{\hat{\sigma}_{signal\ ,i}} \tag{3.1}$$

where $\hat{\sigma}^2_{noise}$ is the local estimated noise variance, as in Eq. 3.1, considering the HH subband at the same

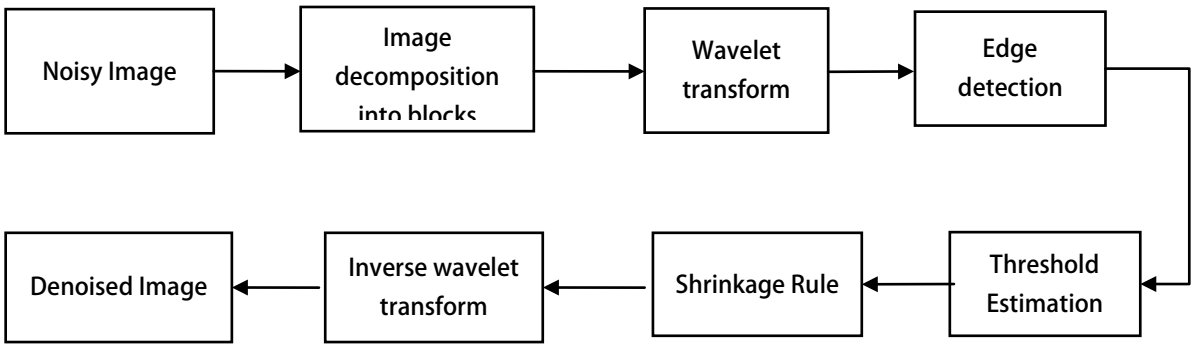

Fig. 1 Block Diagram of Proposed Methodology

decomposition level as the i subband, and $\hat{\sigma}_{signal\ ,i}$ is the local estimated image deviation on the subband under consideration, estimated as

$$\hat{\sigma}_{signal\ ,i} = \sqrt{max(\hat{\sigma}_G^2 - \hat{\sigma}^2{}_{noise}\ , 0)} \tag{3.2}$$

$$\hat{\sigma}_G^2 = \frac{1}{N_S}\sum_{x,y=1}^{N_S} G_{xy}^2 \tag{3.2}$$

and N_S is the number of wavelet coefficients G_{xy} on the subband under consideration.Therefore, the wavelet coefficients are thresholded adaptively according to their subbands. As the decomposition level increases, the coefficients of the subband usually become smoother. For example, the subbandHH_3 is smoother than the corresponding subband in the previous level (HH_2), so the threshold value of HH_3 should be estimated to remove fewer coefficients than the one for HH_2. A shrinkage rule is applied taking into account the threshold according to the edge map. Coefficients related to active edge elements must be associated with smaller threshold values. For such coefficients, the threshold λ_c proposed in our method is computed as the product between the subband threshold λ_i and a given value τ, expressed by

$$\lambda_c = \tau\lambda_i \tag{3.3}$$

that is, τ corresponds to a factor used to weight the threshold in wavelet coefficients related to edges in the image.

Finally, the inverse multiscale decomposition is performed over each external block B_n. The non-overlapping inner blocks B_m are used to reconstruct the denoised image $\hat{f}$ and reduce errors near block boundaries, since the blocks B_m, when concatenated, are much less likely to suffer blocking effects.

IV. SIMULATION RESULTS

The proposed image denoising method, implemented in Matlab, is applied to several test images corrupted with additive Gaussian noise N(0, σ^2) The test set comprises images form Caltech 256 database [2], as well as well known images such as glasses, lightning, window, boat, fingerprint and man. A subset of the images, shown in Fig. 2, is considered in the discussions that follows. Experimental results at different noise levels are reported. The following sections describe the used performance metrics, the experimental setup for the proposed method and comparisons to other denoising approaches. Approximates it best, under given evaluation criteria. A common criterion is minimizing the mean-squared error(MSE), which is defined for gray-scale images as

$$MSE = \frac{1}{M\times N}\left\|f-\hat{f}\right\|^2 = \frac{1}{M\times N}\sum_{x=1}^{M}\sum_{y=1}^{N}\left(f_{xy}-\hat{f}_{xy}\right)^2 \qquad (4.1)$$

Another common performance measure based on MSE is the peak image to noise ratio (PSNR), which is defined in decibels (dB) for 8-bit gray-scale images as

$$PSNR = 10log_{10}\left(\frac{255^2}{MSE}\right) \qquad (4.2)$$

A critical issue with the MSE (or PSNR) is that it does not measure the resulting image quality directly and it can attribute similar scores to images with large differences in psycho visual quality. The structural similarity index (SSIM) [9] was proposed as a metric to compare images which correlates more appropriately with the human perception. It maps two images into an index in the interval [- 1, 1], where higher values are given to more similar pairs of images A and B, calculated as

$$SSIM(A,B) = \frac{(2\mu_A\mu_B+c_1)(2\sigma_{AB}+c_2)}{(\mu_A^2+\mu_B^2+c_1)(\sigma_A^2+\sigma_B^2+c_2)} \qquad (4.3)$$

where μ_A, μ_B, σ_A^2 and $\sigma_B^2$are the averages and variances of A and B, σ_{AB} is the covariance between A and B, and both $c_1$and c_2 are predefined constants.

Pratt's figure of merit (FOM) [3] is widely employed to objectively rate the quality of edge detection, defined as

$$FOM = \frac{1}{\max(N_1+N_D)}\sum_{1}^{N_D}\frac{1}{1+\alpha d_i^2} \qquad (4.4)$$

where N_1 and N_D are the numbers of ideal and detected edge pixels, respectively, α is an empirical constant (often 1/9) used to penalize displaced edges and d_i represents the distance between an edge point and the nearest ideal edge pixel. The value of FOM is a number in the interval [0, 1], where 1 represents the better performance, that is, the detected edges coincide with the ideal edges

(a)

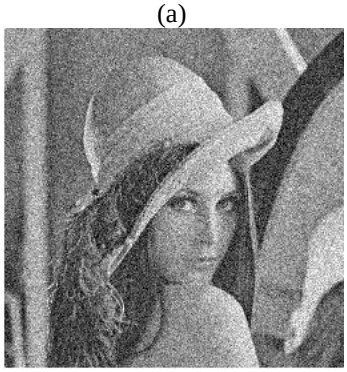

(b)

(c)

Figure 2 (a) Lenna Original, (b) Noisy Image, (c) Denoised Image

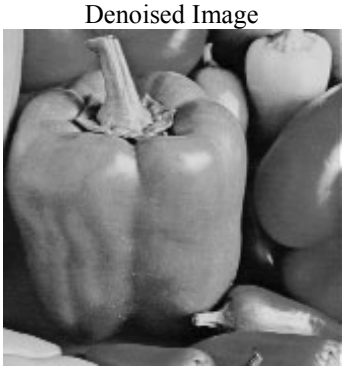

(a)

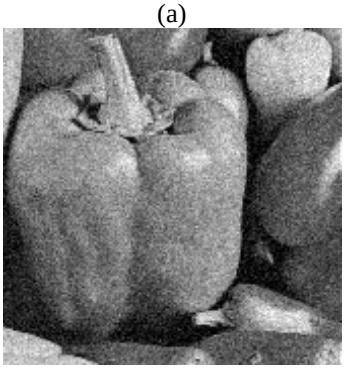

(b)

(c)

Figure 3 (a) Pepper Original, (b) Noisy Image, (c) Denoised Image

Table 1 PSNR of Proposed Method

	PSNR (In dB)	
Noise Density	**Lenna**	**Pepper**
10	42.3037	37.4960
20	32.5617	31.9964
30	30.3303	29.1987
35	28.9535	28.4877
40	28.3374	27.9953

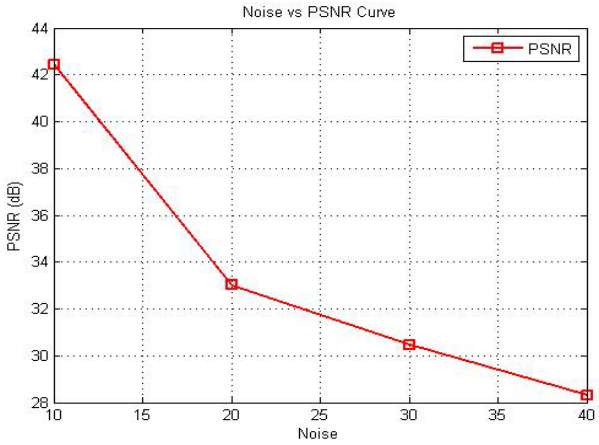

Fig: 4 PSNR Vs Noise graph of Lenna image for proposed method

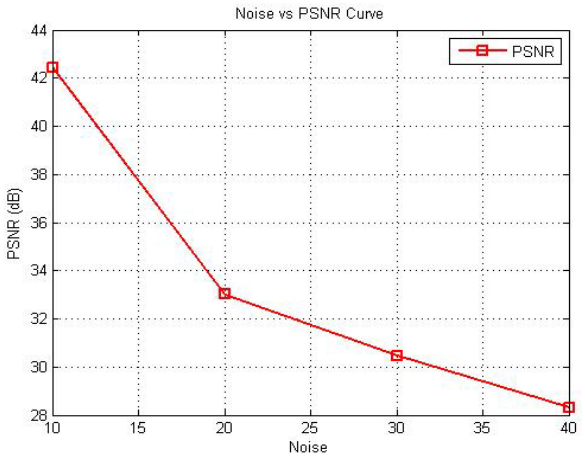

Fig: 5 PSNR Vs Noise graph of Lenna image for proposed method

V. EXPERIMENTAL SETUP

We estimate a set of parameters used by the proposed method: wavelet transform and its number of decomposition levels, block sizes, shrinkage rule and τ (Eq. 19). To perform these estimations, a set of images, different from those shown in the comparisons, was used. Once the parameters are set, they are kept fixed throughout the comparisons to other methods. A set of stationary wavelets [2] from Symlet, Coiflet, Daubechies and Biorthogonal families is tested for A set of stationary wavelets [3] from Symlet, Coiflet, Daubechies and Biorthogonal families is tested for effectiveness. According to our experiments, Daubechies-3 (db3) provided better results than other wavelet bases. Thus, all wavelet-based methods (Bayes, Bivariate, Adaptive) used the Daubechies-3 wavelet for comparison purpose. In addition, four decomposition levels achieved the best results and will be considered in the remaining experiments. Different block sizes are considered in the experiments.. Large blocks allow effective removal of low-frequency noise, but tend to smooth details. Tests revealed that blocks with sizes up to 64 × 64 pixels encompassing blocks sized a multiple of their size preserve sharp characteristics and avoid blockiness.

Based on the results obtained, shown in Fig. 15, blocks of size 64 × 64 pixels encompassing blocks of size 16 × 16 provided slightly better results than the other block sizes (considering PSNR and SSIM) and will be used during the comparisons. According to our experiments, the best value for τ, defined in Eq. 3.19, is 0.8. This shows that it is worth having a trade-off between smoothness and edge preservation. This value will be used in the remaining experiments and comparisons. Finally, a comparison among different shrinkage rules used in our denoising method is shown in Fig. 4. The PSNR value obtained for each shrinkage rule corresponds to an average calculated over a subset of all images used in our experiments. The soft shrinkage rule, given in Eq. 3.15, is clearly superior to other schemes and, therefore, it is chosen over other described rules to threshold coefficients in our experiments.

Comparisons

To assess the denoising effectiveness, the proposed method is compared to state-of-the-art methods. Namely, Bayes, Sure [5] Vishu [4], Oracle, Neigh, Smooth which are wavelet-based. PSNR (in dB) values of the denoised images relative to their original images using such methods are reported in Tables 2 . The best values for wavelet-based methods are clearly shown that proposed meyhod gives highest PSNR values. The right-most column in table show the results of wavelet-based denoising based on adaptive thresholding method. The results obtained by the proposed method reveal significant gain when compared with such

methods, specially considering Bayes and Sure methods. The proposed method achieves similar results to all approaches considered in the comparison. However, when only wavelet-based approaches are considered, the proposed method achieves better results with PSNR and FOM and is similar to the Bays method regarding the SSIM measure.

Even though the proposed method is simple in nature, the results are comparable to those obtained with Bays and superior to vishu, Sure, Oracle and Neigh. Compared to Bays, it is worth noticing that, although this method behaves well for lower noise ratios, it experiences a downfall at two higher noises (σ = 30 and σ = 35). Differently, the proposed method presents a more linear trend. Bayes wavelet-based methods tend to produce smoothed results in homogeneous regions. Nevertheless, certain features such as edges are affected. As the proposed denoising method takes into account the located edges in each high frequency sub and to threshold the wavelet coefficients, it is possible to observe that such adaptive thresholding, in conjunction with the block approach, effectively reduces noise while preserving features of the image. The Sure method produces a similar result on edges.

The proposed method outperforms Sure in homogeneous regions, producing smoother results. The Sure, Vishu and Neigh methods fail to smooth images when noise increases to higher levels. Bays produces good results at lowerr values but obtains poor denoised images at higher noise levels.

Oracle and Neigh methods output smoothed images. The worst resulting images are produced at higher levels of noise. The Sure method shows a general tendency for over smoothing which leads to images with an oil painting like effect.

Table 2 Comparison of Peak Signal to Noise Ratio (PSNR) for Different Noise Densities and Images

Noise	**PSNR**						
	Vishu shrink	**Sure shrink**	**Bayes shrink**	**Oracle shrink**	**Neigh shrink**	**Smooth shrink**	**Proposed Method**
Lena							
σ = 10	30.56	33.47	33.41	33.61	34.45	30.41	39.25
σ = 20	28.75	30.07	30.22	30.38	30.11	27.43	29.96
σ = 30	26.78	28.39	28.49	28.60	27.69	24.88	27.23
σ = 35	25.41	27.82	27.85	27.94	26.76	23.8	26.05
σ = 40	18.25	21.55	21.57	22.02	21.97	19.07	23.02
Pepper							
σ = 10	27.72	30.63	31.03	31.50	32.92	25.87	37.47
σ = 20	24.91	27.29	27.28	27.40	28.57	23.19	29.25
σ = 30	24.61	25.09	25.28	25.32	26.11	20.84	27.19
σ =35	23.99	24.22	24.52	24.58	25.27	19.82	26.45
σ =40	19.23	20.26	21.04	21.15	21.97	17.54	22.24

VI. CONCLUSIONS

This method presented an adaptive edge-preserving image denoising method in wavelet domain. A new thresholding scheme is proposed based on noise estimation on high frequency sub ands and edge strength. The choice of thresholding functions integrated with edge detection can improve the performance of denoising methods. Results indicated that the proposed method effectively suppresses Gaussian noise without smoothing important image details. Experiments demonstrated that the new method produces superior results compared to other methods based on the wavelet transform and results comparable to other state-of-the-art denoising methods.

REFERENCES

[1] Abreu E, Lighstone M, Mitra S, Arakawa K (1996) A new efficient approach for the removal of impulsive noise from highly corrupted images. IEEE Trans Image Process 5(6):1012–1025

[2] Garnett R, Huegerich T, Chui C, He W (2005) A universal noise removal algorithm with an impulse detector. IEEE Trans Image Process 14(11):1747–1754

[3] Gonzalez RC, Woods RE (2006) Digital image processing. Prentice-Hall, Upper Saddle River

[4] Pitas I, Venetsanooulos A (1990) Nonlinear digital filters: principles and applications, Kluwer, Boston

[5] Yu¨ksel M, Bastu¨rk A (2003) Efficient removal of impulse noise from highly corrupted digital images by a simple neuro-fuzzy operator. Int J Electron Commun 57(3):214–219

[6] Sethian JA (1999) Level set methods and fast marching methods: evolving interfaces in computational geometry, fluid mechanics, computer vision and materials sciences. Cambridge University Press, Cambridge

[7] Chambolle A, Vore RD, Lee NY, Lucier B (1998) Nonlinear wavelet image processing: variational problems, compression, and noise removal through wavelet shrinkage. IEEE Trans Image Process 7(3):319–335

[8] Chambolle A (2004) An algorithm for total variation minimization and applications. J Math Imaging Vis 20(1–2):89–97

[9] Rudin L, Osher S, Fatemi E (1992) Nonlinear total variation based noise removal algorithms. Phys D 60:259–268

[10] Black MJ, Sapiro G, Marimont DH, Heeger D (1998) Robust anisotropic diffusion. IEEE Trans Image Process 7(3):421–432

[11] Katkovnik V, Egiazarian K, Astola J (2006) Local approximation techniques in signal and image processing, vol. PM157, SPIE Press, USA

[12] Weickert J, terHaarRomeny BM, Viergever MA (1998) Efficient and reliable schemes for nonlinear diffusion filtering. IEEE Trans Image Process 7(3):398–410.